ISSN 1674-1056
http://cpb.iphy.ac.cn
http://iopscience.iop.org/cpb
中国物理 B
Chinese Physics
中国物理 Chinese Physics B

First-principles study of the $(Cu_xNi_{1-x})_3Sn$ precipitations with different structures in Cu-Ni-Sn alloys

Guang-Wei Peng(彭广威), Xue-Ping Gan(甘雪萍), Zhou Li(李周), Ke-Chao Zhou(周科朝)

Citation: Chin. Phys. B . 2018, 27(8): 086302. **doi:** 10.1088/1674-1056/27/8/086302

Journal homepage: http://cpb.iphy.ac.cn; http://iopscience.iop.org/cpb

What follows is a list of articles you may be interested in

Superconductivity in electron-doped arsenene

Xin Kong(孔鑫), Miao Gao(高淼), Xun-Wang Yan(闫循旺), Zhong-Yi Lu(卢仲毅), Tao Xiang(向涛)

Chin. Phys. B . 2018, 27(4): 046301. **doi:** 10.1088/1674-1056/27/4/046301

Magnetism and piezoelectricity of hexagonal boron nitride with triangular vacancy

Lu-Si Zhao(赵路丝), Chun-Ping Chen(陈春平), Lin-Lin Liu(刘林林), Hong-Xia Yu(于洪侠), Yi Chen(陈怡), Xiao-Chun Wang(王晓春)

Chin. Phys. B . 2018, 27(1): 016301. **doi:** 10.1088/1674-1056/27/1/016301

First-principles analysis of the structural, electronic, and elastic properties of cubic organic-inorganic perovskite $HC(NH_2)_2PbI_3$

Jun-Fei Wang(王俊斐), Xiao-Nan Fu(富笑男), Jun-Tao Wang(王俊涛)

Chin. Phys. B . 2017, 26(10): 106301. **doi:** 10.1088/1674-1056/26/10/106301

First-principles investigations on the mechanical, thermal,electronic, and optical properties of the defect perovskites Cs_2SnX_6 (X= Cl, Br, I)

Hai-Ming Huang(黄海铭), Zhen-Yi Jiang(姜振益), Shi-Jun Luo(罗时军)

Chin. Phys. B . 2017, 26(9): 096301. **doi:** 10.1088/1674-1056/26/9/096301

Structural, electronic, and magnetic behaviors of 5d transition metal atom substituted divacancy graphene: A first-principles study

Rafique Muhammad, Yong Shuai(帅永), He-Ping Tan, Hassan Muhammad

Chin. Phys. B . 2017, 26(5): 056301. **doi:** 10.1088/1674-1056/26/5/056301

First-principles study of the $(Cu_xNi_{1-x})_3Sn$ precipitations with different structures in Cu–Ni–Sn alloys*

Guang-Wei Peng(彭广威)[1,2], Xue-Ping Gan(甘雪萍)[1,†], Zhou Li(李周)[3], and Ke-Chao Zhou(周科朝)[1]

[1] *State Key Laboratory of Powder Metallurgy, Central South University, Changsha* 410083, *China*
[2] *Hunan Automotive Engineering Vocational College, Zhuzhou* 412001, *China*
[3] *School of Materials Science and Engineering, Central South University, Changsha* 410083, *China*

(Received 13 March 2018; revised manuscript received 28 April 2018; published online 10 July 2018)

The structural parameters, the formation energies, and the elastic and thermodynamic properties of the $(Cu_xNi_{1-x})_3Sn$ phase with different structures are studied by the virtual crystal approximation (VCA) and super-cell (SC) methods. The lattice constants, formation energies, and elastic constants obtained by SC and VCA are generally consistent with each other. It can be inferred that the VCA method is suitable for $(Cu_xNi_{1-x})_3Sn$ ordered phase calculation. The calculated results show that the equilibrium structures of Cu_3Sn and Ni_3Sn are $D0_a$ and $D0_{19}$ respectively. $(Cu_xNi_{1-x})_3Sn_D0_3$ with various components are the metastable phase at temperature of 0 K, just as $D0_{22}$ and $L1_2$. With the temperature increase, the free energy of the $D0_3$ is lower than those of $D0_{22}$ and $L1_2$, and $D0_{22}$ and $L1_2$ eventually turn into $D0_3$ in the aging process. The $(Cu_xNi_{1-x})_3Sn_D0_{22}$ is first precipitated in a solid solution because its structure and cell volume are most similar to those of a solid solution matrix. The $L1_2$ and the $D0_{22}$ possess better mechanical stability than the $D0_3$. Also, they may play a more important role in the strengthening of Cu–Ni–Sn alloys. This study is valuable for further research on Cu–Ni–Sn alloys.

Keywords: $(Cu_xNi_{1-x})_3Sn$, first-principle, virtual crystal approximation, super-cell

PACS: 63.20.dk, 71.20.Lp, 71.15.Nc **DOI:** 10.1088/1674-1056/27/8/086302

1. Introduction

The Cu–Ni–Sn alloy is a significant material of interest in science and technology due to its high strength, elasticity, and good corrosion and wear resistance.[1,2] Many studies have been performed to understand the precipitation hardening mechanism of the Cu–Ni–Sn alloy.[3,4] It has been proved that $(Cu_xNi_{1-x})_3Sn$ can be formed into five different structures: $D0_{22}$(tI8), $L1_2$ (cP4), $D0_3$(cF16), $D0_a$ (oP8), and $D0_{19}$ (hP8),[5–7] as shown in Fig. 1.

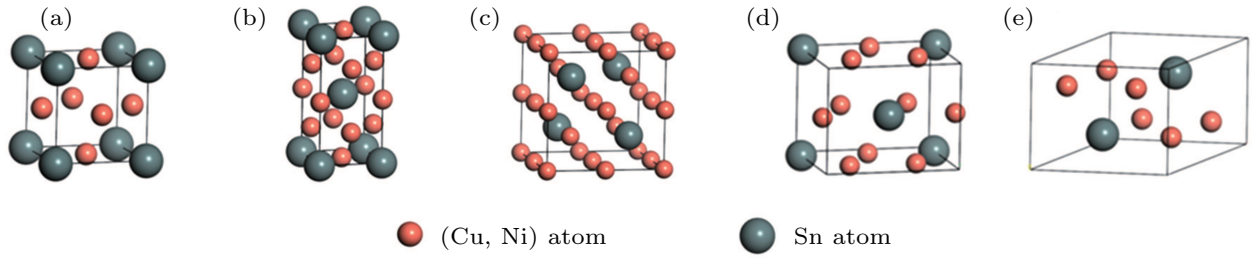


Fig. 1. (color online) Lattice structures of $(Cu_xNi_{1-x})_3Sn$: (a) $L1_2$, (b) $D0_{22}$, (c)$D0_3$, (d) $D0_a$, and (e) $D0_{19}$.

Although the equilibrium structures of Cu_3Sn and Ni_3Sn are $D0_a$ and $D0_{19}$ respectively, $D0_a$ and $D0_{19}$ can be hardly precipitated from a face-centered cubic (fcc) solid solution, in which the atoms do not have enough diffusion capacity to overcome the structural difference in the solid phase transition. The $D0_{22}$, $L1_2$, and $D0_3$ are the main strengthening phases precipitated from the supersaturated solid solution of the Cu–Ni–Sn alloy, as indicated by the experimental time-temperature-transformation (TTT) curves of the Cu–15Ni–8Sn alloy in Fig. 2.[8] When the alloy is aged at a temperature range from about 300 °C to 500 °C, $D0_{22}$ is first precipitated from the α supersaturated solution. As the aging time goes by, $D0_{22}$ will be transformed into $L1_2$, and with the aging time further increasing, both the $D0_{22}$ and $L1_2$ will be transformed into $D0_3$. When the aging temperature increases to a certain extent, atoms obtain a greater diffusion capacity, and $D0_3$ will

*Project supported by the National Key Research and Development Program of China (Grant No. 2016YFB0301402), the Project of Innovation-Driven Plan in Central South University, and the State Key Laboratory of Powder Metallurgy, Central South University, Changsha, China.

†Corresponding author. E-mail: ganxueping@csu.edu.cn

© 2018 Chinese Physical Society and IOP Publishing Ltd

be precipitated from the α supersaturated solution directly.

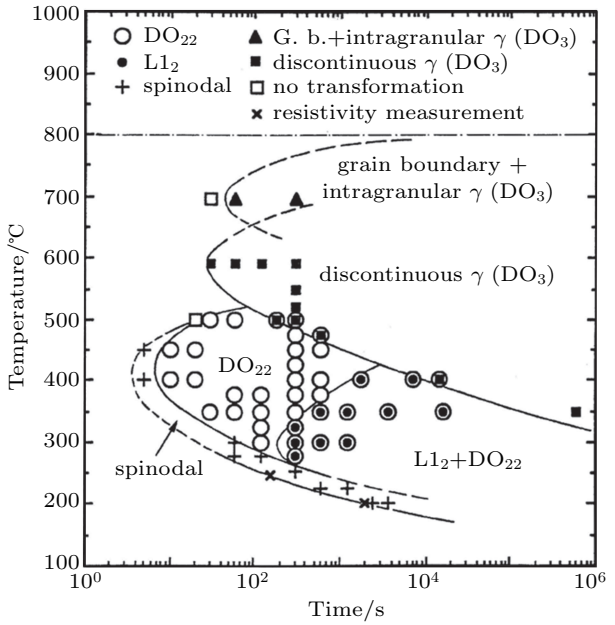


Fig. 2. The time-temperature-transformation (TTT) diagram of the Cu–15Ni–8Sn alloy.[8]

Nevertheless, the compositions, structures, and properties of $(Cu_xNi_{1-x})_3Sn$ with different ordered structures have not yet been fully understood due to the phase transition complexity of the Cu–Ni–Sn system. There has been no systematic study of the $(Cu_xNi_{1-x})_3Sn$ with various structures. The compositions, structural stabilities, and mechanical properties of the $D0_{22}$, the $L1_2$, and the $D0_3$ need to be discussed. Some important fundamental issues arise as follows.

(i) It is generally accepted that Ni only strengthens the matrix by solid solution and does not affect the phase transformation, but some documents indicated that when the content of Sn is constant, the brittleness of the alloy decreases with the increase of the Ni content.[9,10] What role does the Ni play in the $(Cu_xNi_{1-x})_3Sn$ phase? Is there any relationship between the properties of $(Cu_xNi_{1-x})_3Sn$ and the x value?

(ii) As transient ordered phases, $D0_{22}$ and $L1_2$ during the aging of supersaturated solid solution were well established. It has been found that $D0_{22}$ ordering takes place prior to $L1_2$ and $D0_3$, and both $L1_2$ and $D0_{22}$ may co-exist in a Cu–15Ni–8Sn alloy.[11,12] What are the relations and differences between the two metastable phases?

In order to understand the effect of $(Cu_xNi_{1-x})_3Sn$ precipitations in Cu–Ni–Sn alloys, it is necessary to gain more knowledge about the $(Cu_xNi_{1-x})_3Sn$ with different structures and different Ni content. The first principles calculation is a most powerful method to investigate the phase stabilities and properties of these $(Cu_xNi_{1-x})_3Sn$ phases.

In the present study, the lattice constants, elastic properties, and electronic and thermodynamic properties of the $D0_{22}$, $L1_2$, and $D0_3$ are investigated by first-principles calculations. By the use of calculations, certain conclusions drawn from the experiments may be well explained, which consequently assist in optimizing the Cu–Ni–Sn alloy properties in subsequent studies.

2. Calculation method

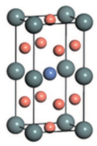
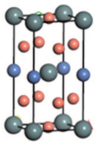
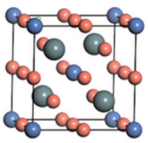
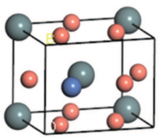
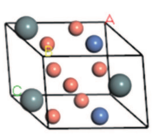
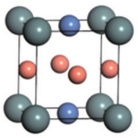
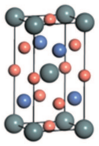
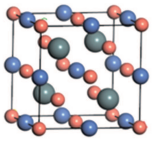
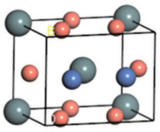
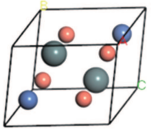
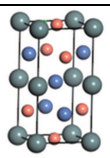
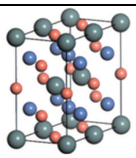
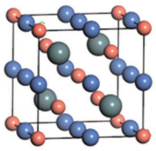
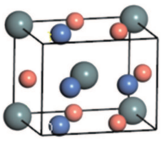
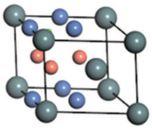
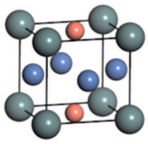
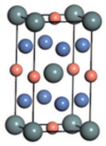
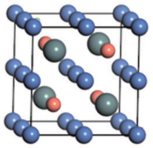
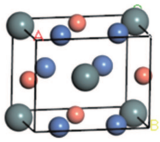
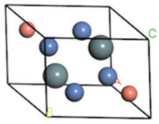
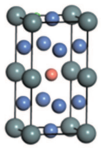
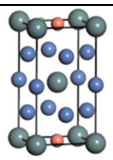
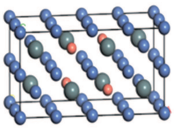
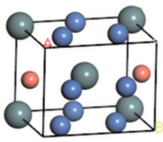
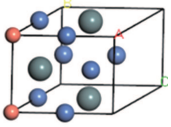
Since the x in $(Cu_xNi_{1-x})_3Sn$ is a variable, neither the Ni content nor the occupation of Ni atoms is definite. Two different calculation methods were used in this work in order to obtain the results that can be compared.

The first method was the super-cell (SC). For a certain composition, the total energies of all possible structures after structural optimization with Ni atoms in different positions were calculated, and the structure with the lowest total energy was identified as the most stable one and taken to the further calculations, and the results are listed in Table 1. In order to simplify the SC structure and save computation time, the x values of $(Cu_xNi_{1-x})_3Sn$ were set to be 1, 5/6, 2/3, 1/2, 1/3, 1/6, and 0, corresponding to the systems of Cu_3Sn, $Cu_{2.5}Ni_{0.5}Sn$, Cu_2NiSn, $Cu_{1.5}Ni_{1.5}Sn$, $CuNi_2Sn$, $Cu_{0.5}Ni_{2.5}Sn$, and Ni_3Sn respectively.

The second method was the virtual crystal approximation (VCA). Since the atomic radius and electronic structure of Ni are very similar to those of Cu, $(Cu_xNi_{1-x})_3Sn$ phases could be treated as a disordered solid solution in the VCA framework, considering the atomic sites in terms of a mixture of atoms that consist of x Cu and $(1-x)$ Ni.[13] In this work, the Cu atoms were taken as mixed atoms with Ni in proportions of 0, 16.667, 33.333, 50, 66.667, 83.333, and 100 at.%, corresponding to the x values of 1, 5/6, 2/3, 1/2, 1/3, 1/6, and 0, respectively.

All calculations were made with the CASTEP program based on density functional theory (DFT). The PW91version of the generalized gradient approximation (GGA) was used in the calculations.[14] The atomic geometry optimizations were performed, with the cutoff energy (E_{cut}) of atomic wave function set to be 440 eV, the convergence tolerance energy 5.0×10^{-6} eV/atom, the Max force 0.01 eV/Å, Max stress 0.02 GPa, and Max displacement 5.0×10^{-4} Å. The Brillouin zone sample integrations used were based on the Monkhorst–Pack grids of 8×8×8-dimensional points for the $L1_2$ structure, 7×7×3-dimensional points for the $D0_{22}$ structure, 7×7×7-dimensional points for the $D0_3$ structure, 5×6×5-dimensional points for the $D0_a$ structure, and 5×5×6-dimensional points for the $D0_{19}$ structure, respectively. All the calculations of phonons properties were based on the "finite displacement" method with the super-cell defined by cutoff radius 5 Å and the dispersion separation was set to be 0.015 1/Å.

Table. 1. (color online) SC structures identified for calculations ($x = 5/6$, 2/3, 1/2, 1/3, 1/6).

x	$L1_2$	$D0_{22}$	$D0_3$	$D0_a$	$D0_{19}$
5/6					
2/3					
1/2					
1/3					
1/6					

3. Results and discussion

3.1. Structural parameters

The calculated equilibrium lattice constants are listed in Table 2. It can be seen that the calculated values of lattice constants are slightly higher than the actual experimental data, which is consistent with the fact that the GGA method usually overestimates the lattice constants.[15] Therefore, the chosen calculation method in this work can be regarded as valid. In Table 1, the calculated lattice constants and the average volumes of atoms by VCA are smaller and closer to the experimental results than those by SC. It indicates that in the (Cu, $Ni)_3Sn$ phases, the Cu and Ni atoms tend to be irregularly distributed so that a more compact arrangement can be obtained.

Table 2. Calculated equilibrium lattice constants, average volumes of atoms, and total energies of different structures.

x	System	Method	Lattice constants/Å		Average volume per atom/Å^3
			This work	Reference	
1	$Cu_3Sn_L1_2$	SC	$a = 3.889$		14.705
	$Cu_3Sn_D0_{22}$	SC	$a = 3.905$, $c = 7.698$		14.673
	$Cu_3Sn_D0_3$	SC	$a = 6.177$	6.117[16]	14.730
	$Cu_3Sn_D0_a$	SC	$a = 5.535$, $b = 4.324$, $c = 4.899$	$a = 5.618$, $b = 4.367$, $c = 4.835$[17] $a = 5.529$, $b = 4.323$, $c = 4.775$[18] $a = 5.49$, $b = 4.32$, $c = 4.74$[19]	14.690
	$Cu_3Sn_D0_{19}$	SC	$a = 5.610$, $c = 4.312$		14.674
5/6	$Cu_{2.5}Ni_{0.5}Sn_L1_2$	VCA	$a = 3.887$		14.167
		SC	$a = 3.810$, $c = 3.963$		14.382
	$Cu_{2.5}Ni_{0.5}Sn_D0_{22}$	VCA	$a = 3.859$, $c = 7.611$		14.168
		SC	$a = 3.822$, $c = 7.863$		14.358
	$Cu_{2.5}Ni_{0.5}Sn_D0_3$	VCA	$a = 6.108$		14.242
		SC	$a = 6.130$		14.397
	$Cu_{2.5}Ni_{0.5}Sn_D0_a$	VCA	$a = 5.511$, $b = 4.296$, $c = 4.812$		14.241
		SC	$a = 5.514$, $b = 4.305$, $c = 4.846$		14.379
	$Cu_{2.5}Ni_{0.5}Sn_D0_{19}$	VCA	$a = 5.551$, $c = 4.272$		14.250
		SC	$a = 5.569$, $c = 4.281$		14.372

Table 2. (*Continued*).

x	System	Method	Lattice Constants/Å		Average volume per atom/Å^3
			This work	Reference	
2/3	$Cu_2NiSn_L1_2$	VCA	$a = 3.812$	$a = 5.984$[20]	13.848
		SC	$a = 3.769$, $c = 3.947$		14.113
	$Cu_2NiSn_D0_{22}$	VCA	$a = 3.855$, $c = 7.444$		13.828
		SC	$a = 3.905$, $c = 7.391$		14.088
	$Cu_2NiSn_D0_3$	VCA	$a = 6.051$		13.847
		SC	$a = 6.086$		14.089
	$Cu_2NiSn_D0_a$	VCA	$a = 5.382$, $b = 4.343$, $c = 4.757$		13.899
		SC	$a = 5.529$, $b = 4.339$, $c = 4.690$		14.064
	$Cu_2NiSn_D0_{19}$	VCA	$a = 5.454$, $c = 4.319$		13.907
		SC	$a = 5.495$, $c = 4.321$		14.124
1/2	$Cu_{1.5}Ni_{1.5}Sn_L1_2$	VCA	$a = 3.790$		13.610
		SC	$a = 3.801$, $c = 3.838$		13.862
	$Cu_{1.5}Ni_{1.5}Sn_D0_{22}$	VCA	$a = 3.851$, $c = 7.342$		13.610
		SC	$a = 3.919$, $b = 3.967$, $c = 7.129$		13.854
	$Cu_{1.5}Ni_{1.5}Sn_D0_3$	VCA	$a = 6.017$		13.615
		SC	$a = 6.056$		13.882
	$Cu_{1.5}Ni_{1.5}Sn_D0_a$	VCA	$a = 5.398$, $b = 4.328$, $c = 4.676$		13.656
		SC	$a = 5.521$, $b = 4.349$, $c = 4.613$		13.845
	$Cu_{1.5}Ni_{1.5}Sn_D0_{19}$	VCA	$a = 5.398$, $c = 4.321$		13.629
		SC	$a = 5.448$, $c = 4.315$		13.864
1/3	$CuNi_2Sn_L1_2$	VCA	$a = 3.774$	$a = 5.934$[18]	13.438
		SC	$a = 3.842$, $c = 3.695$		13.637
	$CuNi_2Sn_D0_{22}$	VCA	$a = 3.818$, $c = 7.374$		13.444
		SC	$a = 3.884$, $c = 7.225$		13.624
	$CuNi_2Sn_D0_3$	VCA	$a = 5.996$		13.473
		SC	$a = 6.025$		13.669
	$CuNi_2Sn_D0_a$	VCA	$a = 5.398$, $b = 4.313$, $c = 4.625$		13.460
		SC	$a = 5.485$, $b = 4.361$, $c = 4.551$		13.608
	$CuNi_2Sn_D0_{19}$	VCA	$a = 5.382$, $c = 4.286$		13.439
		SC	$a = 5.386$, $c = 4.325$		13.584
1/6	$Cu_{0.5}Ni_{2.5}Sn_L1_2$	VCA	$a = 3.762$		13.311
		SC	$a = 3.804$, $c = 3.718$		13.450
	$Cu_{0.5}Ni_{2.5}Sn_D0_{22}$	VCA	$a = 3.808$c=7.355	$a = 3.77$c=7.24[21]	13.332
		SC	$a = 3.856$, $c = 7.235$		13.454
	$Cu_{0.5}Ni_{2.5}Sn_D0_3$	VCA	$a = 5.980$		13.365
		SC	$a = 6.000$		13.500
	$Cu_{0.5}Ni_{2.5}Sn_D0_a$	VCA	$a = 5.359$, $b = 4.300$, $c = 4.621$	$a = 5.493$, $b = 4.30$, $c = 4.513$[18]	13.311
		SC	$a = 5.424$, $b = 4.311$, $c = 4.594$	$a = 5.380$, $b = 4.285$ $c = 4.495$[22]	13.428
	$Cu_{0.5}Ni_{2.5}Sn_D0_{19}$	VCA	$a = 5.353$, $c = 4.285$		13.291
		SC	$a = 5.364$, $c = 4.294$		13.374
0	$Ni_3Sn_L1_2$	SC	$a = 3.763$	$a = 3.738$[19]	13.321
	$Ni_3Sn_D0_{22}$	SC	$a = 3.846$, $c = 7.213$		13.352
	$Ni_3Sn_D0_3$	SC	$a = 5.984$	$a = 5.982$[18] $a = 5.980$[19]	13.392
	$Ni_3Sn_D0_a$	SC	$a = 5.377$, $b = 4.288$, $c = 4.629$		13.341
	$Ni_3Sn_D0_{19}$	SC	$a = 5.357$, $c = 4.280$	$a = 5.286$, $c = 4.243$[7] $= 5.305$, $c = 4.254$[18] $a = 5.327$, $c = 4.269$[22]	13.296

The average volumes per atom as a function of composition x are presented in Fig. 3. The average volumes of $(Cu_xNi_{1-x})_3Sn$ phases with $L1_2$, $D0_{22}$, $D0_3$, $D0_a$, and $D0_{19}$ structures show negative deviation from Vegard's law, and the volumes from the VCA deviate more from those from Vegard's law than those from the SC. It implies that the attraction between Cu and Ni atoms is greater than that between the atoms of the same kind, and the VCA method is more suitable for the calculation of the alloy than the SC method.

The volume comparison among the five different structures is shown in Fig. 4. Although there is a difference between the calculated volumes from SC and VCA, the volumes of the five structures show roughly the same variation tendency. With the

same x value, the volumes of the $D0_{22}$ are the smallest in all structures in the period of $1 \geq x \geq 1/2$. It can therefore explain the case appearing in the experiment[8] that the first phase precipitated from the α supersaturated solid solutions at a lower temperature is the $D0_{22}$. Since at low temperature, the activity of atoms is limited, and the precipitation of $D0_{22}$ leads to the smallest matrix distortion.

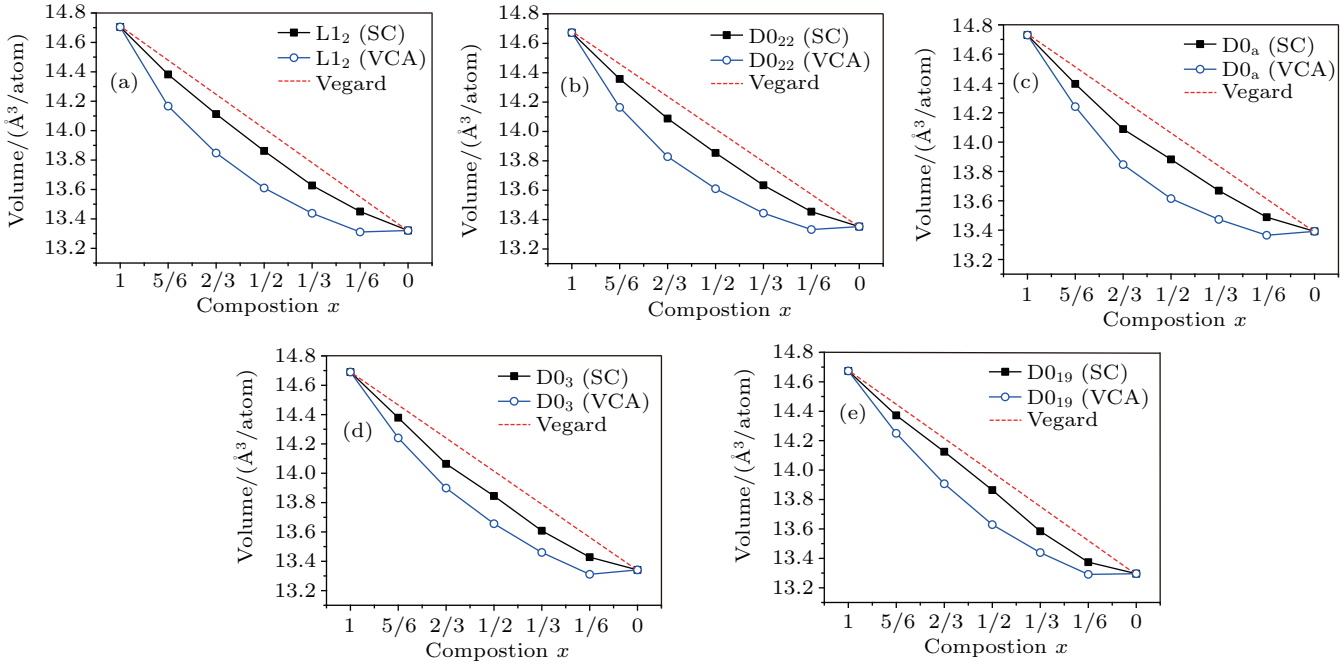


Fig. 3. (color online) Calculated average volumes per atom of $(Cu_xNi_{1-x})_3Sn$ for (a) $L1_2$, (b) $D0_{22}$, (c) $D0_3$, (d) $D0_a$, and (e) $D0_{19}$.

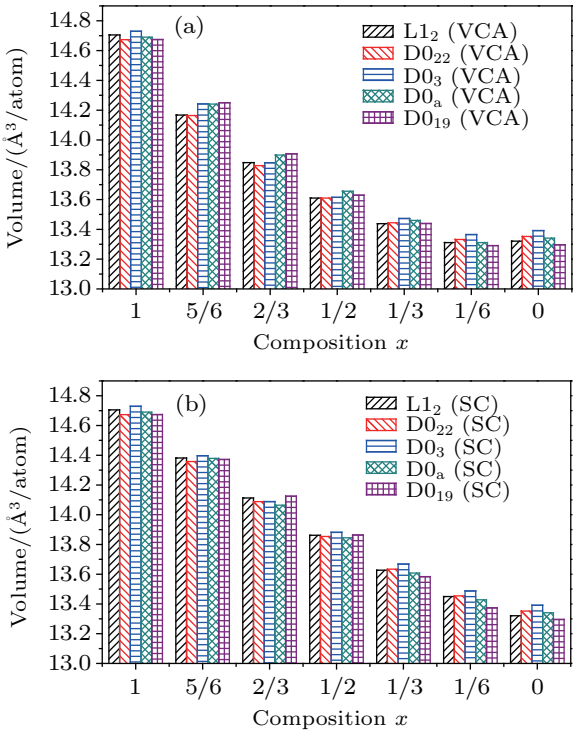


Fig. 4. (color online) Calculated average volumes per atom of $(Cu_xNi_{1-x})_3Sn$ (a) by SC method and (b) VCA method.

3.2. Formation energies

The calculations of formation energies are performed to compare the stabilities among the $L1_2$, $D0_{22}$, $D0_3$, $D0_a$, and $D0_{19}$ structures.

For the ordered super-cell structure, the formation energy of the Cu–Ni–Sn alloy is defined as follows:[23]

$$\Delta\bar{H} = \frac{1}{x+y+z}(E_{\text{tot}} - xE^{\text{Cu}}_{\text{solid}} - yE^{\text{Ni}}_{\text{solid}} - zE^{\text{Sn}}_{\text{solid}}), \quad (1)$$

where $\Delta\bar{H}$ is the average formation energy per atom, E_{tot} is the total energy of the unit cell, $E^{\text{Cu}}_{\text{solid}}$ is the energy per atom of Cu with a face-centered cubic (fcc) structure, $E^{\text{Ni}}_{\text{solid}}$ is the energy per atom of Ni with the fcc structure, and $E^{\text{Sn}}_{\text{solid}}$ represents the energy per atom of β-Sn in the solid state.

Therefore, the formation energy of $(Cu_xNi_{1-x})_3Sn$ super-cell structure in this work can be written as

$$\Delta\bar{H} = \frac{1}{4}[E_{\text{tot}} - 3xE^{\text{Cu}}_{\text{solid}} - 3(1-x)E^{\text{Ni}}_{\text{solid}} - E^{\text{Sn}}_{\text{solid}}]. \quad (2)$$

As far as the disordered VCA structure is concerned, there is no doubt that equation (2) is unsuitable due to the unreasonable energy standard of the pure element, and the formation energy must be developed by considering the influence of mixture atoms on the formation energy.[24,25] Since the Cu and Ni atoms are treated as virtual mixed atoms, the $xE^{\text{Cu}}_{\text{solid}}$ and $(1-x)$ $E^{\text{Ni}}_{\text{solid}}$ should be replaced by the total energy of Cu_xNi_{1-x} calculated by VCA. Therefore, the formation energy of $(Cu_xNi_{1-x})_3Sn$ VCA structure can be written as

$$\Delta\bar{H} = \frac{1}{4}(E_{\text{tot}} - 3E^{\text{Cu}_x\text{Ni}_{1-x}}_{\text{solid}} - E^{\text{Sn}}_{\text{solid}}), \quad (3)$$

where $E_{\text{solid}}^{Cu_xNi_{1-x}}$ is the energy of the mixed atom in the optimized α-Cu_xNi_{1-x} solution, calculated by the VCA method.

The calculated formation energies of the $(Cu_xNi_{1-x})_3Sn$ alloy are shown in Fig. 5. It can be seen that the results obtained by the two methods are very close to each other, and the variation trend of the formation energies from the VCA is the same as that from the SC. The formation energies of all the structures decrease with Ni atom content increasing. Since the VCA is based on the disorder structure, while SC is based on ordered replacements of Ni in Cu sites, the difference between formation energies obtained by the VCA and SC method can help indicate the tendency of atomic arrangement in different structures. For $L1_2$, $D0_a$, and $D0_{19}$ phases, the formation energies calculated by SC are more negative than those by VCA when $1 > x \geq 2/3$, which indicates that Cu and Ni atoms tend to be ordered. While the opposite scenario occurs when $1/2 \geq x > 0$ as shown in Figs. 5(a), 5(d), and 5(e).

For the $D0_3$ phase, the formation energies calculated by SC are a little more negative than those by the VCA as shown in Fig. 5(c), indicating that the Cu and Ni atoms in $D0_3$ structure prefer to be arranged regularly. By comparing the formation energies among the $D0_3$ supercellular structures with different atomic arrangements, an interesting rule is found. The body-central positions are prone to be occupied by Cu atoms rather than Ni atoms, since this kind of atomic arrangement possesses a more compact structure with lower energy. For example, the energy-lowest structure of Cu_2NiSn is $D0_3$, but the energy-lowest structure of $CuNi_2Sn$ is $L2_1$ as shown in Fig. 6. These are consistent with the experimental results that the $(Ni,Cu)_3Sn$ alloys have both $D0_3$ and $L2_1$ structures.[26] It may be explained that the sizes of Cu and Sn atoms are more close than those of Ni and Sn atoms, and the more compact structures with lower formation energies can be formed with Cu atoms at the body-central positions.

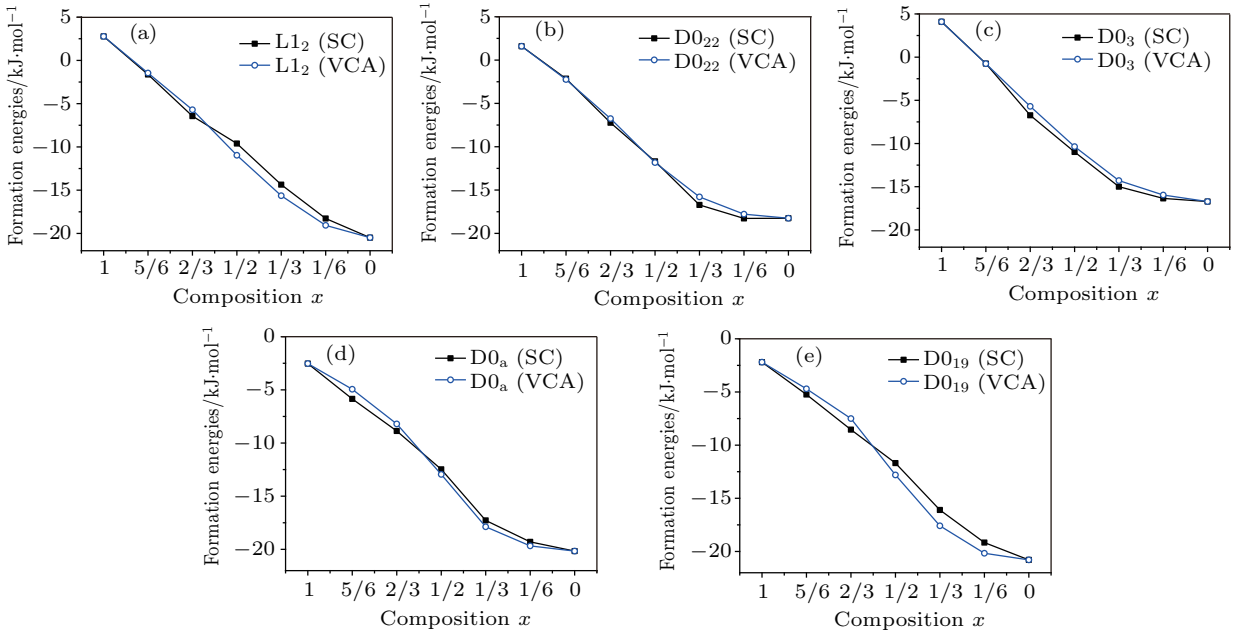


Fig. 5. (color online) Calculated formation energies of $(Cu_xNi_{1-x})_3Sn$ with different structures: (a) $L1_2$, (b) $D0_{22}$, (c) $D0_3$, (d) $D0_a$, and (e) $D0_{19}$.

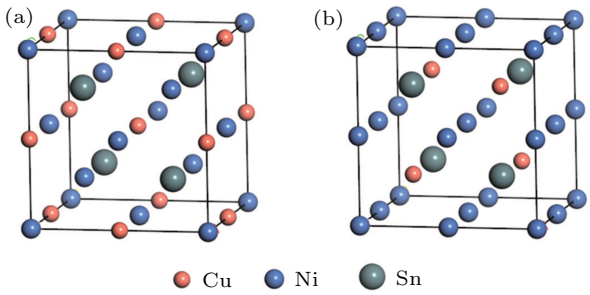


Fig. 6. (color online) Energy-lowest structures of $(Cu_xNi_{1-x})_3$–$D0_3$: (a) Cu_2NiSn and (b) $CuNi_2Sn(L2_1)$.

The formation energies comparisons of the five different structures are shown in Fig. 7. When $x = 1$, the formation energies of $L1_2$, $D0_{22}$, and $D0_3$ are all positive, indicating that Cu_3Sn compounds with these structures are very difficult to form. The $D0_a$ and $D0_{19}$ phases possess the negative formation energies, and the formation energy of $D0_a$ is lowest, so the equilibrium phase structure of Cu_3Sn should be $D0_a$. When $x = 0$, the formation energy of $D0_{19}$ is lowest, indicating that the equilibrium phase structure of Ni_3Sn should be $D0_{19}$. These results are consistent with those in the literature.[27] However, because of the structural difference, it is difficult for $D0_a$ and $D0_{19}$ to precipitate directly from the fcc solid solution matrix. With a comprehensive analysis of structures and formation energies, the structure of the $(Cu_xNi_{1-x})_3$ first precipitated from the α supersaturated solid solution should be $D0_{22}$. As time goes by, the $D0_{22}$ phase with high Ni content will be transformed into $L1_2$.

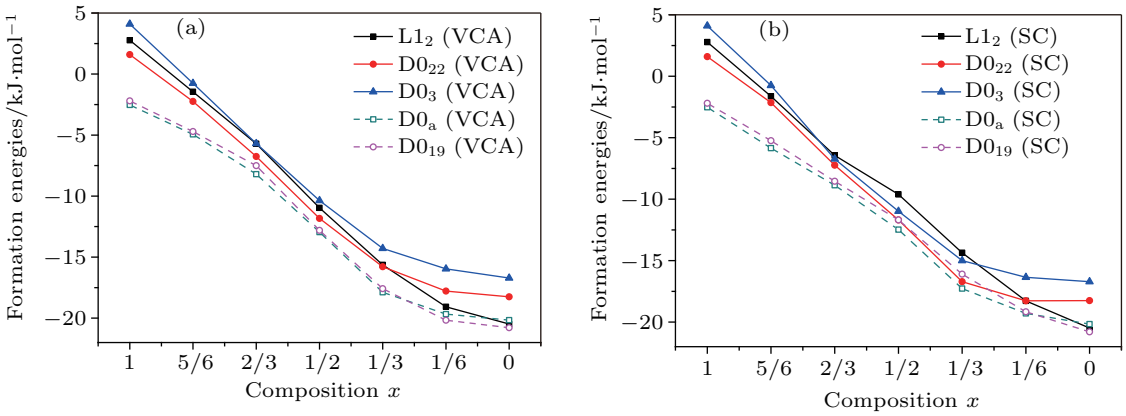


Fig. 7. (color online) Calculated formation energies of $(Cu_xNi_{1-x})_3$ by (a) SC method and (b) VCA method.

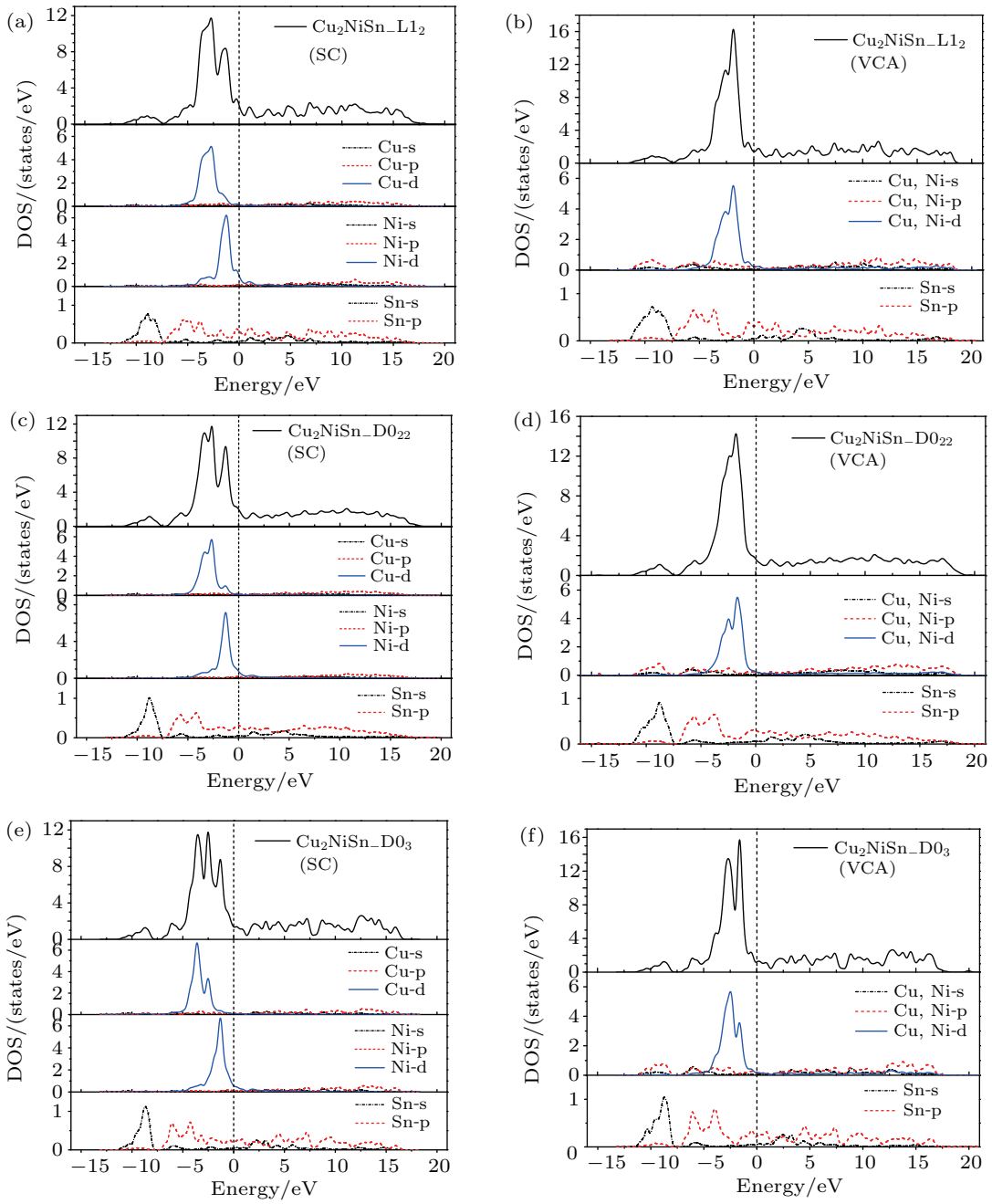


Fig. 8. (color online) TDOSs and PDOSs of $(Cu_xNi_{1-x})_3Sn$ with different structures, with Fermi level set to zero.

3.3. Electronic structure

To confirm the validity of the VCA method and further reveal the underlying mechanisms of the structural stability for the $(Cu_xNi_{1-x})_3Sn$ phases, the electronic total and partial densities of states (TDOSs and PDOSs) at equilibrium lattice constants for Cu_2NiSn are calculated by the VCA and SC method, respectively, and the results are shown in Fig. 8. The Fermi energy level is set to be zero on the x axis. It can be seen that the Cu_2NiSn compounds with $L1_2$, $D0_{22}$, and $D0_3$ structures exhibit metallic behaviors because the values of TDOS at the Fermi level are higher than 0. TDOSs of Cu are very similar to those of Ni in all the figures of various structures, which indicates that the Cu and Ni have similar electronic structures and properties in the $(Cu_xNi_{1-x})_3Sn$. The TDOSs are mainly dominated by Cu-d (the energy of PDOS peak is in a range from about -4.8 eV to -1.0 eV) or Ni-d (the energy of PDOS peak is in a range from about -4.2 eV to 0 eV). As seen from the PDOSs of Figs. 8(a), 8(c), and 8(e), the Cu-d states show strong hybridizations with Ni-d states. It can be seen by comparing Fig. (a) with Fig. 8(b) that the peak of TDOS calculated by the VCA method is narrower and higher than that of TDOS calculated by the SC method, although their positions are roughly the same. It can be explained that in the calculation by the VCA, the PDOSs of mixed (Cu,Ni) atoms are the average of the respective PDOSs of Cu and Ni.

3.4. Mechanical properties

Generally, the elastic constants are closely related to the mechanical behaviors of the materials and also provide information regarding bonding characteristics. The requirement of mechanical stability leads to the following restrictions of the elastic constants,[28] for cubic unit cells

$$C_{11} > |C_{12}|, \quad C_{44} > 0, \quad C_{11} + 2C_{12} > 0; \tag{4}$$

for tetragonal crystals[29]

$$C_{11} > |C_{12}|, \ C_{44} > 0, \ C_{66} > 0, \ (C_{11} + C_{12})C_{33} > 2C_{13}^2. \tag{5}$$

Table 3. Calculated values of elastic constants C_{ij} (in unit GPa), modulus (in unit GPa), and Poisson's ratio of $(Cu_xNi_{1-x})_3Sn$.

x	Structure	Method	C_{11}	C_{12}	C_{13}	C_{33}	C_{44}	C_{66}	B	G	E	G/B	ν
1	$L1_2$	SC	207.2	91.3	–	–	56.4	–	129.9	57.0	149.2	0.44	0.31
	$D0_{22}$	SC	136.0	103.0	94.7	141.3	44.7	41.2	110.9	31.7	86.8	0.29	0.37
	$D0_3$	SC	182.7	121.0	–	–	79.4	–	141.5	54.4	144.7	0.38	0.33
5/6	$L1_2$	VCA	154.7	111.3	–	–	27.1	–	122.5	35.9	98.1	0.29	0.37
		SC	154.1	130.6	93.0	181.8	54.2	60.5	124.7	37.3	101.8	0.30	0.36
	$D0_{22}$	VCA	125.0	97.9	81.4	158.3	50.2	67.1	108.2	38.6	103.5	0.36	0.34
		SC	157.7	113.8	83.8	179.2	55.0	49.1	114.5	41.4	110.8	0.36	0.34
	$D0_3$	VCA	125.6	111.9	–	–	71.0	–	116.5	30.2	83.4	0.26	0.38
		SC	136.4	115.7	–	–	79.9	–	121.0	32.5	89.5	0.27	0.38
2/3	$L1_2$	VCA	120.6	107.1	–	–	64.8	–	118.3	41.9	112.4	0.35	0.34
		SC	146.0	98.5	120.7	182.4	66.2	46.8	121.6	45.1	120.4	0.37	0.33
	$D0_{22}$	VCA	158.7	74.9	102.3	134.2	61.6	60.1	113.3	43.2	115.0	0.38	0.33
		SC	177.3	91.5	136.0	142.0	64.1	60.4	124.9	46.4	123.9	0.37	0.33
	$D0_3$	VCA	126.2	96.6	–	–	80.5	–	106.5	42.0	111.4	0.39	0.33
		SC	162.0	122.6	–	–	88.0	–	125.8	44.8	120.1	0.36	0.34
1/2	$L1_2$	VCA	161.3	93.3	–	–	60.8	–	122.3	46.7	124.3	0.38	0.33
		SC	177.9	112.3	109.6	184.4	68.4	63.8	134.7	49.3	131.8	0.37	0.34
	$D0_{22}$	VCA	158.9	68.7	96.3	129.8	67.0	37.3	107.8	41.5	110.3	0.38	0.33
		SC	186.6	125.9	123.6	179.0	63.8	59.7	134.2	46.4	124.8	0.35	0.34
	$D0_3$	VCA	93.9	142.3	–	–	78.0	–	126.1	–39.0	–130.4	–0.31	0.67
		SC	96.6	145.5	–	–	77.9	–	126.8	–37.1	–123.3	–0.29	0.66
1/3	$L1_2$	VCA	175.6	97.6	–	–	54.7	–	125.2	49.0	130.0	0.39	0.33
		SC	198.3	106.0	114.9	182.9	66.2	65.2	140.1	56.6	149.6	0.40	0.32
	$D0_{22}$	VCA	200.5	112.7	125.4	157.0	73.9	72.0	141.9	50.8	136.2	0.36	0.34
		SC	209.4	115.7	133.3	193.8	71.8	58.7	153.0	53.0	142.5	0.35	0.34
	$D0_3$	VCA	121.1	137.8	–	–	72.8	–	132.3	14.5	42.0	0.11	0.45
		SC	139.6	149.3	–	–	81.1	–	146.1	16.7	48.3	0.11	0.44
1/6	$L1_2$	VCA	215.2	111.7	–	–	72.8	–	149.6	64.6	169.4	0.43	0.31
		SC	217.9	122.1	118.7	242.5	74.4	81.3	155.1	66.0	173.4	0.43	0.31
	$D0_{22}$	VCA	193.9	115.0	130.2	169.1	77.6	67.7	145.2	55.4	147.4	0.38	0.33
		SC	220.2	108.7	133.2	211.0	76.1	66.3	155.6	59.9	159.3	0.38	0.33
	$D0_3$	VCA	144.7	152.6	–	–	98.2	–	150.0	23.5	67.0	0.16	0.43
		SC	148.5	153.2	–	–	91.1	–	158.3	27.4	77.7	0.17	0.42
0	$L1_2$	SC	232.9 227.0[a]	118.9 125.3[a]	–	–	92.6 95.6[a]	–	156.9 159.2[a]	76.2 74.2[a]	196.7	0.49	0.29
	$D0_{22}$	SC	240.7	121.7	140.5	209.0	91.3	72.2	166.1	66.3	175.5	0.40	0.32
	$D0_3$	SC	147.4 151.4[a]	163.7 169.7[a]	–	–	94.3 99.8[a]	–	158.3	17.7	51.2	0.11	0.45

[a] Calculated results in Ref. [34]

The bulk modulus (B) is the measure of unit cell incompressibility, and shear modulus (G) reflects material resistance to the shear strain. Young's modulus (E) is the comprehensive index of the B and G, which reflects the material stiffness and an internal property of the material.[30] Poisson's ratio (ν) is used to quantify the stability of the crystal against shear, and the larger the ν, the better the plasticity is. These polycrystalline structural properties are important for determining the mechanical properties of materials and can be calculated by using the Voigt–Reuss–Hill (VRH) approximation[31] from the following formulas:

$$B = B_{\rm H} = (B_{\rm V} + B_{\rm R})/2, \quad G = G_{\rm H} = (G_{\rm V} + G_{\rm R})/2,$$
$$E = 9BG/(3B+G), \quad \nu = (3B - 2\,G)/(3B+G). \qquad (6)$$

Generally, the ductility of a material can be estimated by the Cauchy pressure value (C_{12}–C_{44}).[32] If the Cauchy value has a positive sign, the material is ductile and displays metallic characteristics, otherwise the material is brittle. Alternatively, the Pugh ratio (G/B) reflects the ductility of alloys.[33] The smaller the Pugh ratio, the more ductile the alloy will be, and the 0.57 ratio is the critical point of all brittle/ductile behaviors.

The mechanical properties of $(Cu_xNi_{1-x})_3Sn$, calculated by SC and VCA are shown in Table 3.

As it is observed in Table 3, the elastic constants of all the $L1_2$ and $D0_{22}$ structures meet the restrictions of mechanical stability. The $D0_3$ structures with $x \leqslant 0.5$ are mechanically unstable since none of their elastic constants meets the restriction of the condition $C_{11} > |C_{12}|$. The Cauchy pressures (C_{12}–C_{44}) of all structures are positive, and all the calculated Pugh ratios (G/B) are less than 0.57. These criteria indicate that $D0_{22}$, $L1_2$, and $D0_3$ structures with various compositions each possess a favorable ductility.

Figure 9 shows the calculated values of Young's modulus (E) and Poisson's ratio (ν) of different structures with different x values. With Ni content increasing, the E value of $L1_2$ and $D0_{22}$ increase while ν decreases, and $D0_3$ presents roughly the opposite scenario. It indicates that $L1_2$ and $D0_{22}$ play a more important role in the strengthening of Cu–Ni–Sn alloys than $D0_3$.

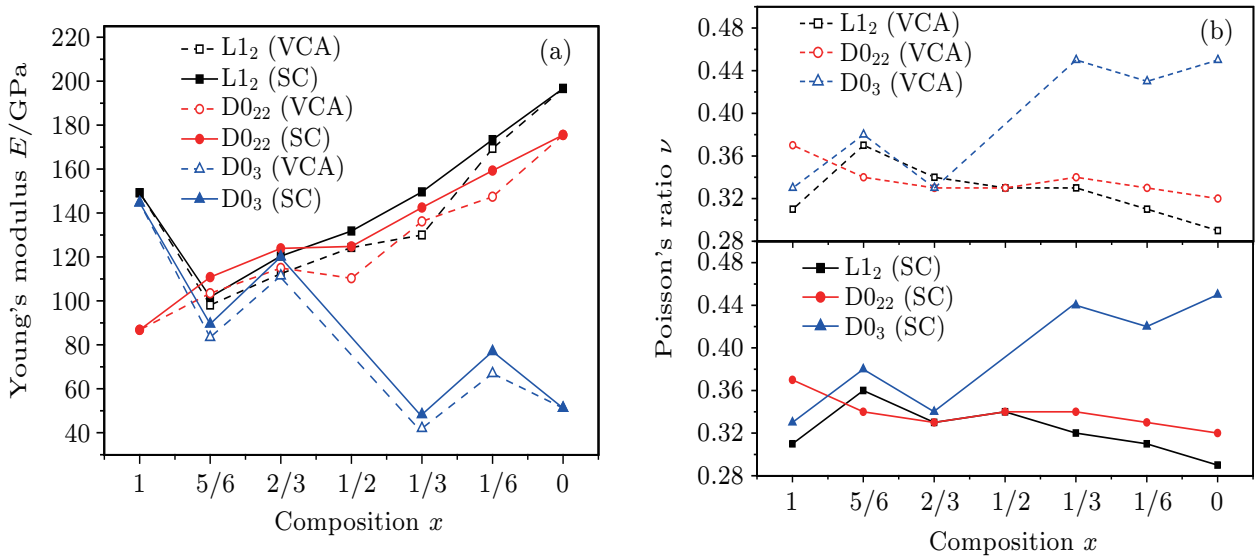


Fig. 9. (color online) Mechanical properties of different structures: (a) Young's moduli and (b) Poisson's ratios.

3.5. Thermodynamic properties

In order to predict the thermodynamic properties of $(Cu_xNi_{1-x})_3Sn$, phonon dispersions are calculated by the SC method. The phonon dispersion curves of $(Cu_xNi_{1-x})_3Sn$ (x = 1, 2/3, 1/3, 0) with $L1_2$, $D0_{22}$, and $D0_3$ structures are shown in Fig. 10. It can be seen from the figure that there are no imaginary frequencies for all the structures, this indicates that they are stable phases.

Figure 11 shows the predicted thermodynamic properties of $(Cu_xNi_{1-x})_3Sn$. It can be clearly found that each of the thermal entropies always has a higher value than enthalpies at all temperatures, resulting in the free energies decreasing with the rise of the temperature. However, the decreasing rates of free energies are not the same. In a range from $x = 1$ to $x = 0$, the free energies of the $D0_3$ are lower than those of $D0_{22}$ and $L1_2$, and the free energy of $Cu_2NiSn_D0_3$ is the lowest in the free energies of all the compounds $(Cu_xNi_{1-x})_3Sn$ as shown in Fig. 10(b). The free energies of the $L1_2$ are lower than those of $D0_{22}$ in all x range values except $x = 1$. This may explain why $D0_{22}$ and $L1_2$ eventually turn into $D0_3$ in the aging process.

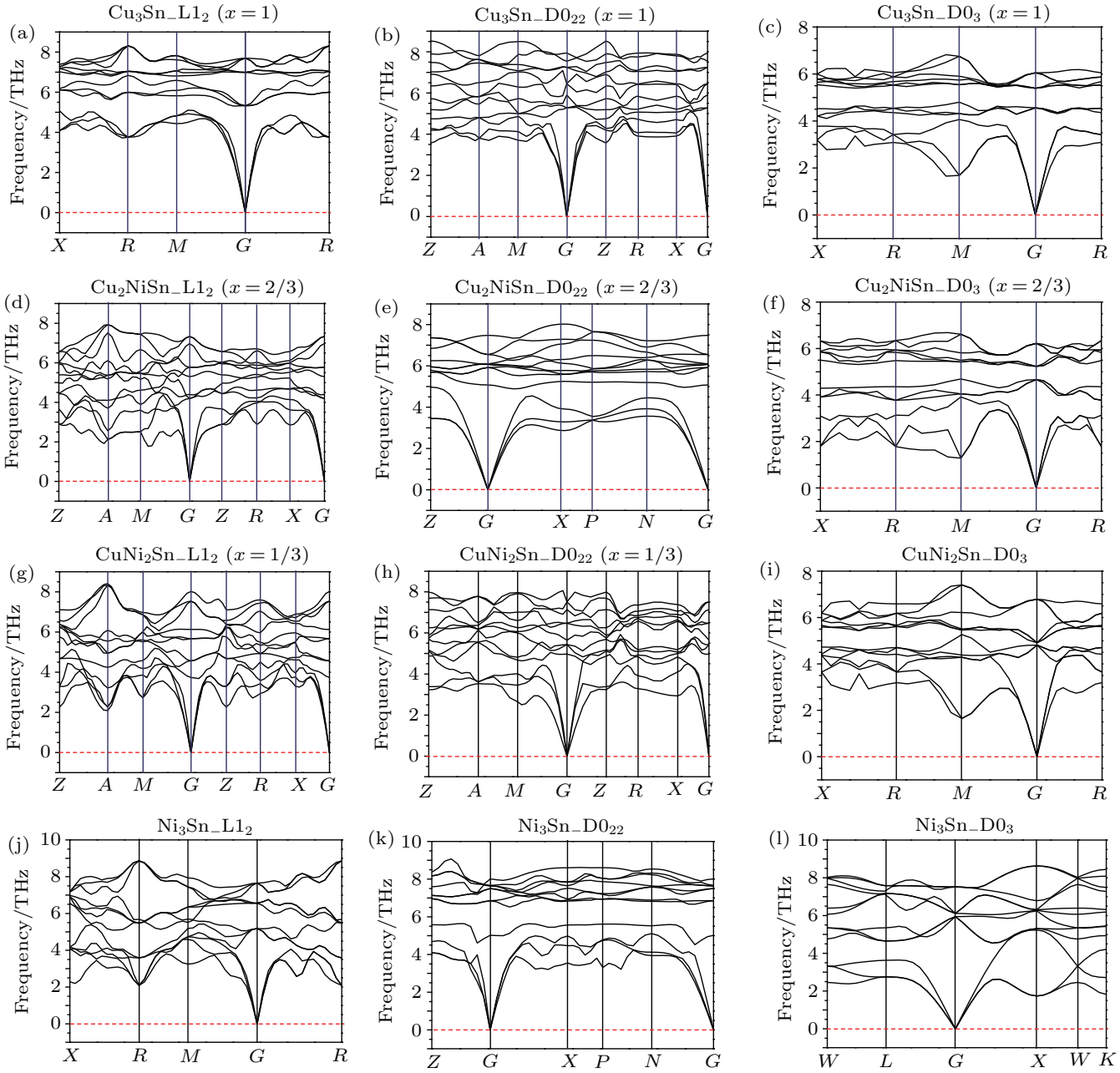
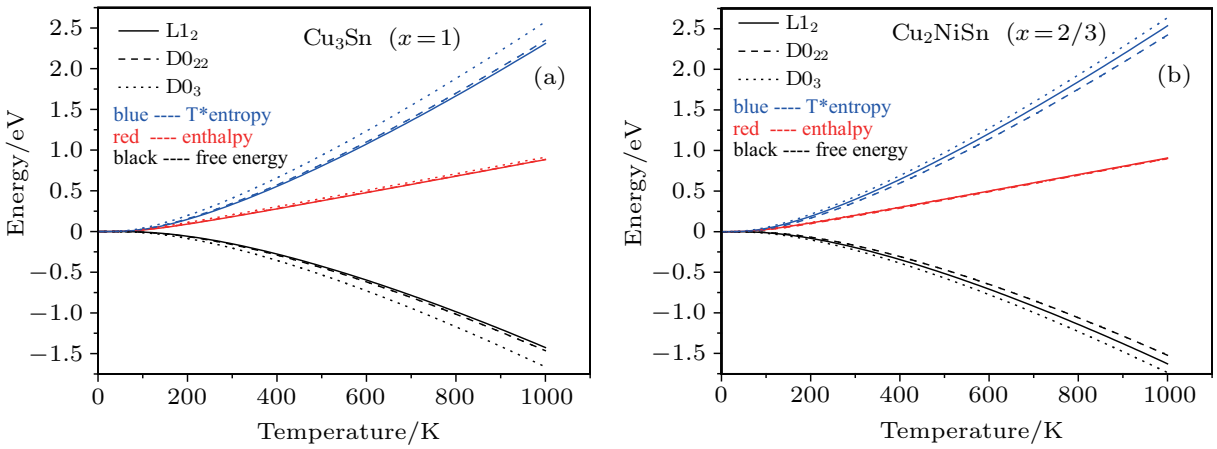


Fig. 10. (color online) Phonon dispersion curves for $(Cu_xNi_{1-x})_3Sn$.



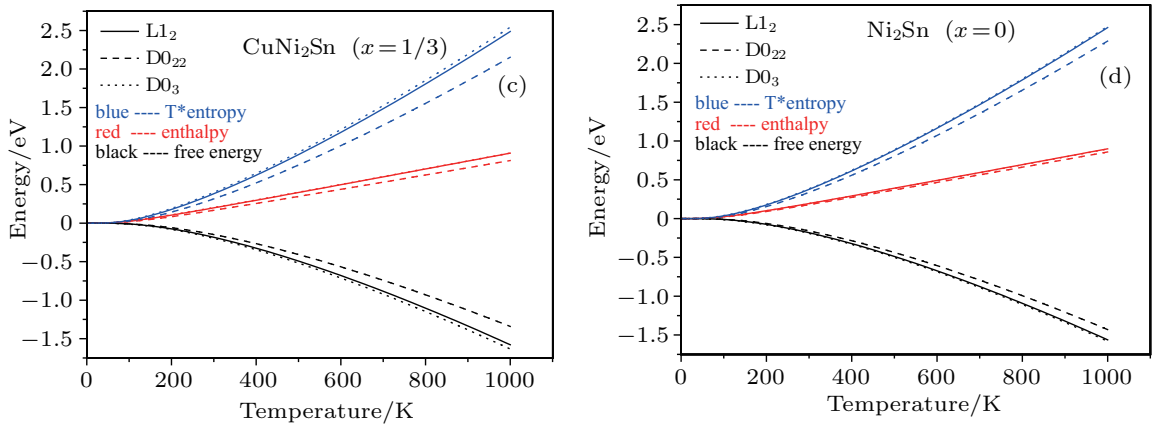


Fig. 11. (color online) Thermodynamic properties calculated by super-cell method.

4. Conclusions

(i) For Cu–Ni–Sn alloys, VCA is a very effective calculation method. It can greatly reduce the amount of calculation and provide the high computational efficiency. The lattice constants, formation energies, and elastic constants obtained by SC and VCA are generally consistent with each other. The density of states shows that the Cu and Ni have similar electronic structures and properties in the $(Cu_xNi_{1-x})_3Sn$, and the TDOSs are mainly dominated by the electron valence of Cu(d) or Ni(d).

(ii) The $(Cu_xNi_{1-x})_3Sn_D0_{22}$ is first precipitated in a solid solution because its structure and cell volume are most similar to those of a solid solution matrix. The $L1_2$ and the $D0_{22}$ possess better mechanical stability than the $D0_3$, and they may play a more important role in the strengthening of Cu–Ni–Sn alloys.

(iii) The calculated results show the equilibrium structures of Cu_3Sn and Ni_3Sn are $D0_a$ and $D0_{19}$ respectively. While $(Cu_xNi_{1-x})_3Sn_D0_3$ with various components are metastable phases at temperature of 0 K, just as $D0_{22}$ and $L1_2$. Nevertheless, with the temperature increasing, the free energy of the $D0_3$ is lower than those of $D0_{22}$ and $L1_2$, and the $D0_{22}$ and $L1_2$ eventually turn into the $D0_3$ in the aging process.

(iv) A comparison among the formation energies of the $D0_3$ supercellular structures with different atomic arrangements shows that the body-central positions are prone to be occupied by Cu atoms rather than Ni atoms, since this kind of atomic arrangement possesses a more compact structure with lower energy. The energy-lowest structure of Cu_2NiSn is $D0_3$, but the energy-lowest structure of $CuNi_2Sn$ is $L2_1$, which is in good consistence with the experimental results that the $(Ni,Cu)_3Sn$ alloys have both $D0_3$ and $L2_1$ structures.

(v) All the calculated results are in good agreement with the previous experimental data, and this study has been shown to be valuable for further research on the Cu–Ni–Sn alloys.

References

[1] Sadykov F A, Barykin N P and Aslanyan I R 1999 *Wear* **225** 649
[2] Ma X C, He G Q, He D H, Chen C S and Hu Z F 2008 *Wear* **265** 1087
[3] Gu D D, Shen Y F and Lu Z J 2009 *Materials Des.* **30** 2099
[4] He D H and Manory R 2001 *Wear* **249** 626
[5] Masamichi Miki and Yoshikiyo Ogino 1961 *J. Jpn. Inst. Met.* **25** 593
[6] Kratochvil P, Mencl J, Pesicka J, *et al.* 1984 *Acta Metall.* **32** 1493
[7] Gupta K P 2000 *J. Phase Equilibria* **21** 479
[8] Shin-ichiro K D, Akinori M and Kento O 2015 *Jpn. Inst. Met. Mater.* **79** 664 (in Japanese)
[9] Wang Y H, Wang M P and Hong B 2004 *Transactions of Materials and Treatment Proceeding of the* 14*th Ifhtse Congress* **25** 97
[10] Plewes J T 1975 *Metall. Trans.* **6A** 537
[11] Zhao J C and Notis M R 1998 *Acta Mater.* **46** 4203
[12] Ahn S and Tsakalakos T 1983 *MRS Proc.* **21** 539
[13] Yu C, Liu J Y, Lu H, Li P L and Chen J M 2007 *Intermetallics* **15** 1471
[14] Perdew, J P, Chevary, J A, Vosko, S H, Jackson, K A Pederson M R, Singh, D J and Fiolhais C 1992 *Phys. Rev. B* **46** 6671
[15] Boulechfar R, Meradji H, Ghemid S, Drabia S and Bouhafs B 2013 *Solid State Sci.* **16** 1
[16] Sadi F and Servant C 2007 *Journal of Thermal Analysis and Calorimetry* **90** 319
[17] Pang X Y, Wang S Q, Zhang L, Liu Z Q and Shang J K 2008 *J. Alloys Compd.* **466** 517
[18] Schreiner W H, Pureur P, Grandi T A, Kunzler J V, BrandÃO D E 1979 *Journal of Thermal Analysis* **17** 489
[19] Sobczak R 1981 *Journal of Magnetism and Magnetic Materials* **24** 325
[20] Schreiner W H , Pureur P, Grandi T A, Kunzler J V and Brandas D E 1979 *J. Therm. Anal.* **17** 489
[21] Lee J S Pak, Mukherjee K, Inal O T and Pak H R 1989 *Mater. Sci. Eng. A* **117** 167
[22] Leepak J C and Inal K 2008 *Choice Reviews Online* **45** 45
[23] Wang T F, Chen P, Deng Y H and Tang B Y 2011 *Transactions of Nonferrous Metals Cociety Society of China* **21** 388
[24] Boulechfar R, Meradji H, Ghemid S, Drablia S and Bouhafs B 2013 *Solid State Sci.* **16** 1
[25] Zhang C S, Yan M F, You Y, Chne H T, Zhang F Y, Bai B, Chen L, Long Z and Li R W 2014 *J. Alloys Compd.* **615** 854
[26] Divis M 1992 *Phys. Stat. Sol. (b)* **173** 13
[27] Yuichiro Murakami and Sukeji Kachi 1983 *Transactions of the Japan Institute of Metals* **24** 9
[28] Hu H, Wu X Z, Wang R, Jia Z H, Li W G and Liu Q 2016 *J. Alloys Compd.* **666** 185
[29] Liu Y Z, Jiang Y H and Zhou R 2014 *Rare Met. Mater. Eng.* **43** 2903
[30] Zhang C L 2001 *Taiyuan University Technology* 2011 (in Chinese)
[31] Nong Z S and Zhu J C 2012 *Physica B* **407** 3555
[32] Pettifor D G 1992 *Mater. Sci. Technol.* **8** 345
[33] Pugh S F 1954 *Philos. Mag.* **45** 823
[34] Li L H, Wang W L and Wei B 2015 *Comput. Mater. Sci.* **99** 274